The reaction of lithium with carbon dioxide studied by photoelectron spectroscopy

ARTICLE *in* SURFACE SCIENCE · NOVEMBER 1998

Impact Factor: 1.93 · DOI: 10.1016/S0039-6028(98)00710-9

ELSEVIER

Surface Science 418 (1998) 139–149

surface science

The reaction of lithium with carbon dioxide studied by photoelectron spectroscopy

Guorong Zhuang [a], Yufeng Chen [b], Philip N. Ross, Jr.[a,*]

[a] *Chemical Sciences Division, Lawrence Berkeley National Laboratory, University of California, Berkeley, CA 94720, USA*
[b] *Material Science Division, Lawrence Berkeley National Laboratory, University of California, Berkeley, CA 94720, USA*

Received 26 February 1998; accepted for publication 13 August 1998

Abstract

The interaction of CO_2 with clean Li at 120–320 K was studied using photoelectron spectroscopy. To assist in the interpretation of the spectra, the C 1s and O 1s core-level binding energies of various Li cluster compounds were calculated using an ab initio SCF method. To further understand the reaction pathway, we also studied the reaction of CO_2 with an O_2 pre-dosed Li surface, and the adsorption of CO on clean Li. The principal reactions occurring between CO_2 (1–30 L) and Li at 120–320 K are: $CO_2 \Rightarrow [CO_2]_{ads}$, $2[CO_2]_{ads} \Rightarrow CO_3^{2-} + CO_{ads}$, probably via an oxalate, $[C_2O_4]_{ads}$, intermediate, and: $CO_{ads} \Rightarrow C + O^{2-}$, $CO_2 + O^{2-} \Rightarrow CO_3^{2-}$. The relative rates of these reactions are temperature dependent. At 120 K, the main products are CO_3^{2-}, CO_{ads}, and $[CO_2]_{ads}$, whereas at 320 K the main products are O^{2-} and elemental carbon with a relatively small amount of CO_3^{2-}. The reactions are similar to those on the other alkali metals, Na, K and Cs, with the important exception being the much stronger interaction with CO, leading to dissociation and carbon formation.

Keywords: Carbonate; Carbon dioxide; Carbon monoxide; Lithium; Peroxide; Photoelectron spectroscopy; Superoxide; Surface chemical reaction

1. Introduction

There are now numerous reports in the battery literature [1–6] that the cycling efficiency of Li electrodes in CO_2-containing electrolyte solutions, such as those made with propylene carbonate (PC), ethylene carbonate (EC) and their mixtures as solvents, is higher than in the same electrolyte without CO_2. The mechanism of this enhanced cycling efficiency is, however, far from clear. Using in situ FTIR, Aurbach and Chusid [3] reported that surface films that formed on Li in the presence of CO_2 contain much more Li_2CO_3 than when CO_2 is not present, and attributed the observed cycling efficiency improvements to the superior properties of the predominantly Li_2CO_3 layer. Osaka et al. [5] investigated the role of CO_2 by studying the surface morphology using ex situ scanning electron microscopy, and concluded that CO_2-containing electrolyte produces a smoother surface by preventing dendritic deposition of lithium, via the reaction of freshly deposited Li with CO_2 to form Li_2CO_3. Osaka et al. also reported that the ion and electronic conductivity of the film formed in CO_2-containing electrolyte is higher than that in electrolyte without CO_2. Thus, all the mechanisms to date propose that the formation

* Corresponding author. Fax: +1 510 486 5530; e-mail: pnross@lbl.gov

0039-6028/98/$ – see front matter
PII: S0039-6028(98)00710-9

of Li_2CO_3 by reaction of freshly deposited Li is responsible for enhanced cycling efficiency. The reaction usually proposed is:

$$2Li + 2CO_2 \Rightarrow Li_2CO_3 + CO\ (gas) \quad (1)$$

There are, however, other studies of the reaction of CO_2 with alkali metals that suggest that this reaction is improbable, and that another source of oxygen is needed to produce CO_3^{2-}. Freund and Roberts [7] have recently written an extensive review of CO_2 surface chemistry, but for the alkali metals only Cs is discussed in detail. State-of-the-art UHV studies of the interaction of CO_2 with Na have been published by Freund and coworkers [8,9] and with K by Hoffman and coworkers [10–12]. It should be noted that in most contemporary UHV studies of CO_2 adsorption the emphasis is on transition metal surfaces containing submonolayer coverages of the alkali metal, with the motivation being understanding the role of alkali metal promoters in catalytic reactions involving CO_2. Hence, the studies have focused on Na and K, and to a lesser extent on Cs, which are the promoters used in commercial catalysts, and there are no comparable studies known to us with Li. At submonolayer coverages of alkali metal, CO_2 activation by the alkali atom is well-established, leading to the formation of CO_{ads} via:

$$CO_2 \Rightarrow O_{ads} + CO_{ads} \quad (2)$$

where the CO_{ads} species is on the transition metal and the O_{ads} resides on the alkali atom. When the surface is fully covered by alkali metal, or on the alkali metal multilayer surface, CO_{ads} desorbs from the surface and for Na and K there is clear evidence [8–12] by both UPS and vibrational spectroscopy of formation of CO_3^{2-}, either directly via an oxolate intermediate:

$$2CO_2 \Rightarrow [C_2O_4]_{ads} \Rightarrow CO_3^{2-} + CO \quad (3)$$

or via further reaction of O_{ads} with CO_2:

$$CO_2 + O_{ads} \Rightarrow CO_3^{2-} \quad (4)$$

For Li surfaces, CO_{ads} desorption would, in our view, be a surprising result, as in our studies [13] of ethereal solvents on Li we have never seen an oxygenated decomposition product desorb from the surface at any temperature. Thus, in the case of Li, the exact decomposition pathway for CO_2 seems unclear and could lead to a variety of products rather than simply CO_3^{2-}. For Li batteries, pathways other than Eq. (1) imply that Li_2CO_3, if it is truly the predominant product of the interaction of CO_2 with freshly deposited Li, forms by interaction with another source of oxygen in the electrolyte, e.g. water.

We report here a study in UHV of the interaction of CO_2 with Li using X-ray and VUV photoemission spectroscopy. A clean Li multilayer evaporated onto Ni(111) was dosed with CO_2 at the lowest temperature possible with our manipulator (120–130 K), and X-ray and/or UV photoemission spectra were collected at successively increasing temperature. Based on analyses of the resulting spectra, a surface reaction path is proposed. In addition, quantum chemical calculations were used in making assignment of C 1s and O 1s binding energies to the individual carbon and oxygen atoms in candidate molecules adsorbed on the Li surface, and to help identify the reaction products. We show that the reaction of CO_2 with clean Li does not lead only to CO_3^{2-}, but to a mixture of CO_3^{2-} with O^{2-} and elemental carbon. The nearest to a pure CO_3^{2-} layer is produced by pre-dosing the surface with oxygen.

2. Experimental

All experiments were conducted in a custom-made UHV system reported earlier [13,14]. The excitation photons were created by a dual anode (Mg/Mg) X-ray source operating at 15 kV and 400 W for XPS, and a commercial all-metal He discharge lamp for UPS. During UPS experiments the sample was biased to negative 20 V to enhance the collection efficiency of the low-energy valence photoelectrons. All spectra were acquired with a double-pass cylindrical mirror analyzer (CMA) having an intrinsic energy resolution ($\Delta E/E$) of 1.6% of the pass energy (E). UPS spectra were acquired at 25 eV pass energy while C 1s and O 1s spectra were acquired at 100 eV pass energy. The Li 1s spectra did not appear to provide additional information, and since acquisition times were very long due to the low cross-section, Li 1s spectra were not routinely obtained. The geome-

tries of electron emission/collection were different in XPS and UPS. For UPS, the sample was nearly perpendicular to the centerline of the CMA, with the photon beam at gazing incidence, so that the electron collection is a cone of emission at fixed polar angle, $40 \pm 5^\circ$ from sample normal. For XPS, the sample was 60° from the CMA centerline, so electrons are collected over a broad range of polar (or take-off) angles, from 15 to 75°. The base pressure of the chamber was 1.5×10^{-10} Torr; during XPS acquisition the pressure was typically $< 5 \times 10^{-10}$ Torr and during UPS it was typically 7×10^{-9} Torr, the higher pressure coming from the He in the discharge lamp.

The Ni(111) (99.995+%) single crystal (Monocrystal Company, Cleveland, OH) was polished with alumina power to 0.05 μ, solvent cleaned and brazed onto a molybdenum plate holder on the UHV manipulator. The crystal was cleaned by combination of Ar^+ ion sputtering and thermal annealing to 950 K repeatedly until the contaminants, mainly carbon, sulfur and oxygen, were below the Auger detection limit. Li was vapor deposited on Ni(111) substrate at 140 K to a thickness of typically 30–40 nm. The Li vapor was from a compact effusion-type source [15,16] consisting of a furnace containing a solid Al–Li alloy with Li atomic concentration of about 9% heated to 550–600°C. Compared with evaporation from a Li dispenser (SEAS Getters, Colorado Springs, CO) we used previously, the Al–Li source provides larger total amounts of metallic Li still free from oxygen and carbon contamination and with better reproducibility in the flux. Auger electron spectroscopy (AES) was used to characterize the cleanliness and the thickness of the lithium overlayer.

Research grade carbon dioxide (purity >99.995%), oxygen (purity >99.998%) and carbon monoxide (purity >99.99%) gases were used as received. The purity of these gases was checked by mass spectrometer before conducting experiments. CO and CO_2 were introduced into the chamber through a 1/64 in capillary doser as part of a thoroughly baked dosing line, while oxygen was introduced by backfilling the chamber to 5×10^{-8} Torr via a separate Varian leak valve attached directly to the main chamber. The CO_2 exposed dosing line was thoroughly pumped and baked after CO gas was introduced to avoid CO gas contamination. During dosing the sample was placed 15 mm in front of the doser to reduce the background pressure rise and to avoid desorbed gas from the chamber wall interacting with lithium directly.

3. Computational methods

Ab initio Hartree–Fock self-consistent calculations with the 6-31G(d) basis set were performed on a Cray J-90 using the Gaussian 94 [17] computational package. The spin-restricted Hartree–Fock (RHF) method was used for calculation with closed shell species and the spin-unrestricted Hartree–Fock (UHF) with open shell species. For open shell molecules, two sets of energy levels were produced for spin-up electrons (α) and spin-down electrons (β), respectively. In this case, we use average values of two slightly different energy levels of α and β electrons. For some species, optimized geometries were obtained representing the minimum total energy, and the electron energies were subsequently calculated on the converged geometries with the same basis set. For some species, a fixed geometry was assumed, and these distinctions are discussed in Section 4. We made the assumption that the Koopmans Theorem approximation, that the binding energy of an electron is approximately equal to the negative of the orbital energy of that electron [18], correctly predicts the relative order of binding energy levels within a given molecule. Therefore, the calculated binding energies were used as a tool to make XPS peak assignments to specific atoms in an undissociated molecule. However, one has to be very cautious when extending the above method to binding energy shifts for an atom with the same nearest neighbor configuration but in different molecules, as the differences in extra-atomic relaxation between different molecules can be greater than the chemical shifts.

4. Results

Unexpectedly complex multipeak C 1s and O 1s spectra were obtained for CO_2 exposed lithium surfaces even at temperatures as low as 130 K,

indicating that there are multiple reaction channels open simultaneously. In order to unravel the intricate features in the spectra, we will present first the results from the interaction of CO_2 with a lithium surface pre-dosed with O_2, which produces a simpler product layer with specific chemical states that are easily identified. These same states can then be identified in the CO_2/Li product mix, greatly aiding the identification of all species in the reaction layer.

4.1. O_2 on lithium

Fig. 1 shows the O 1s spectrum obtained after a Li layer was exposed to 1.5 L of O_2 at 130 K. It appears that there exists more than one chemical state of oxygen at this condition. We fit the spectrum with commercial software (PeakFit™, Jandel Scientific) according to the following procedure. The isolated peak at the lowest binding energy was first fit with a Gaussian lineshape and its linewidth (FWHM) was thus determined to be 1.8 eV. The full spectrum was then fitted with all the O states constrained to the same linewidth (FWHM) 1.8 eV. The solid line represents the resulting curve fit to the raw data (dots). The peak positions and relative intensities (from peak areas) are shown as bar graphs superposed on the fitted spectrum. There are three components at binding energies of 534.1, 532.7 and 530.3 eV.

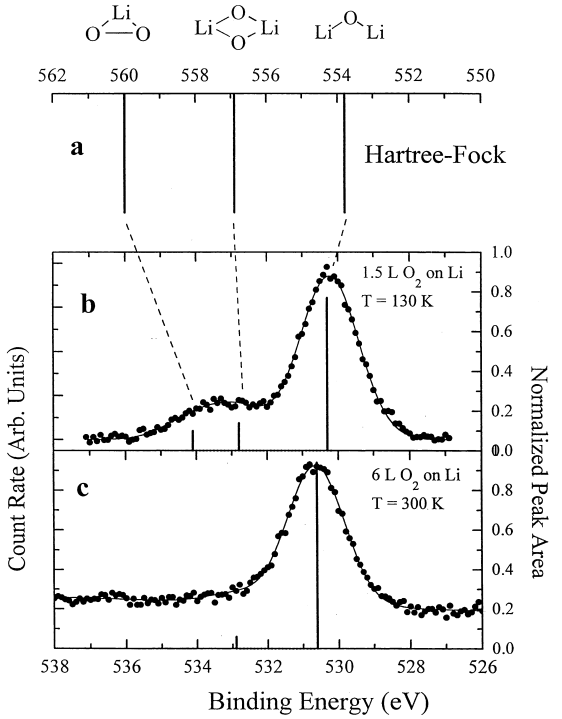

Fig. 1. (a) Koopmans Theory calculation of lithium oxide (Li_2O), lithium peroxide (Li_2O_2) and lithium superoxide (LiO_2) clusters; XP spectra of (b) lithium exposed to 1.5 L of O_2 at 130 K, (c) lithium exposed to 6 L of O_2 at 300 K.

The Koopmans Theorem binding energies of three kinds of Li–O species were calculated by ab initio self-consistent Hartree–Fock method (SCF) method based on converged geometries. The geometry of the species deduced from infrared spectroscopy [19] was used as a starting point of geometry optimization. Two possible forms of lithium superoxide, rhombus and bending, were proposed from infrared spectroscopy. Our calculation suggests that they both have the same total energy and O 1s binding energy level, although the infrared spectrum is indicative of the planar rhombus structure [19]. The calculated O 1s binding energies of the candidate Li_xO_y species shown in Fig. 1a allow us to assign the experimental measured binding energies 534.1, 532.7 and 530.3 eV to lithium superoxide (LiO_2), lithium peroxide (LiO_2Li) and lithium oxide (Li_2O), respectively. These binding energy assignments are essentially identical ($\pm$0.2 eV) to those made earlier for the same species by Qiu et al. [20] using chemical intuition, i.e. the partial ionic character of the bonds and the net charge of oxygen atoms. Dosing the clean Li surface with 6 L of O_2 at 300 K leads to the expected result of only lithium oxide (Fig. 1c).

4.2. CO_2 on O_2 pre-dosed lithium

In order to understand the lithium carbonate formation mechanism, the lithium surface predosed with 1.5 L of O_2 at 130 K (O 1s spectrum shown in Fig. 1) was followed by exposure to 10 L of CO_2 at 120 K.[1] The sample temperature was

[1] Experiments were also done with the lithium surface predosed with 6 L of oxygen with similar results. However, the spectra all show a higher fraction of unreacted oxygen, and since one of our purposes here was to produce as pure a surface carbonate state as possible, we focus on the results with 1.5 L dosing.

then raised using a ramp-and-hold program, with the ramp rate being 5°C/s, and the hold period the time it takes to acquire the C 1s and O 1s spectra for this temperature. A series of C 1s and O 1s spectra acquired as a function of temperature is shown in Fig. 2, along with peak fitting results.

The C 1s spectrum obtained at 120 K shows primarily a single chemical state with binding energy of 292 eV. In the O 1s spectrum, there are three oxygen states at binding energies of 534.0, 533.2, and 530.3 eV. The simplest interpretation of this spectrum is that the state at 530.3 eV is residual oxygen from the original oxide state on the pre-dosed surface, and two states at higher binding energy are created by reaction of the CO_2 with the pre-dosed surface oxygen to form surface carbonate, CO_3^{2-}. The major peak in the C 1s spectrum is thus assigned to surface carbonate, CO_3^{2-}. Definitive evidence that the state at 292 eV in our C 1s spectrum at 120 K is CO_3^{2-} is provided by the He(II) valence band spectrum for the same surface. This is shown in Fig. 3, along with the experimental spectrum for a bulk K_2CO_3 sample by Connor and coworkers [21,22]. We calculated the molecular orbitals for CO_3^{2-} ion using Gaussian 94 with the 6-31G(d) basis set and the same geometry of the ion (D_{3h}) used earlier by Connor and coworkers, and arrived at essentially identical results, as shown in Table 1. D_{3h} is not, however, the exact geometry of the CO_3^{2-} ion in bulk carbonates, and we therefore also made the calculation using the geometry of the ion in lithium carbonate [23], which is still planar but with two different C–O bond distances. The resulting calculated spectrum was not significantly different from that for the D_{3h} geometry. Assuming the relaxation energies are the same for all orbitals, after aligning the $1a_2'$ orbital energy to the first feature in the experimental spectrum, it is clear that the calculated energy levels for the CO_3^{2-} ion match both the experimental spectra, the spectrum of Connor et al. for the bulk carbonate and our spectrum for what we propose is surface carbonate, formed by reaction of CO_2 with pre-dosed oxygen.

While the majority of the carbon on the oxygen

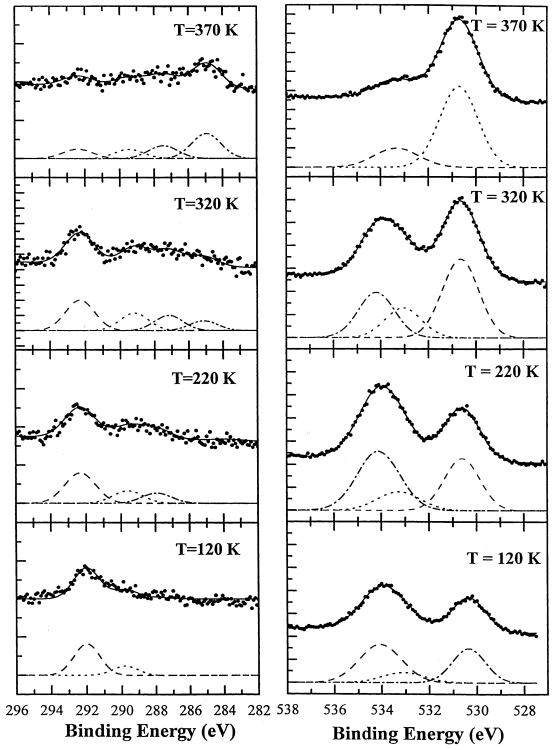

Fig. 2. Series of XP spectra of 1.5 L oxygen predosed surface exposed to 10 L of CO_2 acquired as a function of temperature. Solid line shows the results of peak fitting, with the individual component spectra shown as dashed, dotted and dot–dash curves.

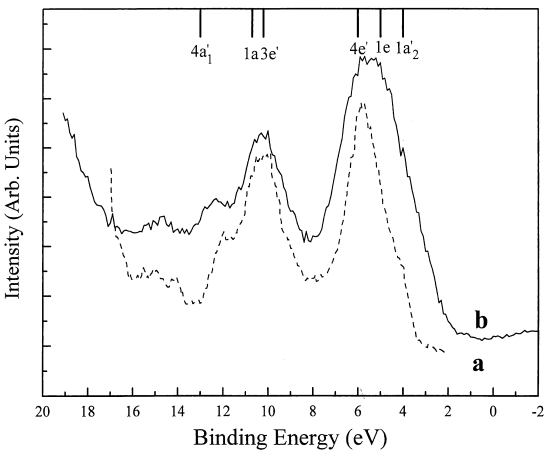

Fig. 3. Comparison of He II UPS of 4 L oxygen pre-dosed surface exposed to 30 L of CO_2 (curve b) with the corresponding spectrum of K_2CO_3 (curve a) [21,22]. Energy levels adjusted to Fermi level of the sample (see text) for the first six molecular orbitals calculated for CO_3^{2-} in bulk Li_2CO_3 (Table 1) are shown.

Table 1
Calculated valence orbital of CO_3^{2-}

Valence orbital	Energy[a] (eV) (STO, D_{3h})	Energy[b] (eV) [6-31G(d), D_{3h}]	Energy[c] (eV) [6-31G(d), in crystal]
$1a_2'$	3.7	3.5	3.4
$1e''$	3.1	2.5	2.4
$4e'$	2.3	1.5	1.6
$3e'$	−2.8	−2.7	−2.6
$1a_2''$	−2.9	−3.2	−3.2
$4a_1'$	−4.9	−5.5	−5.6
$2e'$	−20.2	−20.4	−20.4, −20.3
$3a_1'$	−24.6	−24.5	−24.3

[a] From Refs. [21,22].
[b] Our ab initio calculation with 6-31G(d) basis, adopting geometry after Connor and coworkers [21,22] with C–O bond distance = 1.27 Å.
[c] Our ab initio calculation with 6-31G(d) basis, adopting geometry of CO_3^{2-} in bulk crystal structure of Li_2CO_3 obtained from Ref. [23].

pre-dosed surface following CO_2 exposure at 120 K is in a single chemical state, as CO_3^{2-}, the peak fitting of both the C 1s and O 1s spectra indicates states of carbon and oxygen other than carbonate and oxide, respectively. In order to assign molecular species to these peaks, we used Gaussian 94 calculated C 1s and O 1s binding energies (Table 2) for Li clusters containing CO_3^{2-} and CO_2^{2-}. For the CO_2 case, we used two different coordinations, one with Li bonded only to oxygens, and one with a mixed coordination of oxygen and carbon. These calculations revealed an ordering of C 1s binding energies in accord with chemical intuition, with binding energies decreasing with oxidation state, i.e. $CO_3^{2-} > CO_2^{2-}$. The peak in the C 1s spectrum at 290 eV is assigned to the carbon atom in chemisorbed CO_2, following the relative chemical shifts of the Li clusters in Table 2. As indicated above, the curve fitting of the O 1s spectrum had revealed a peak at 533.2 eV, which we would assign correspondingly to the oxygen in chemisorbed CO_2, which is also consistent with the relative O 1s binding energies of the clusters given in Table 2. From the relative peak areas, the amount of chemisorbed CO_2 at 120 K is about 20–25% of the amount of carbonate.

Table 2
Koopmans Theory binding energies[a] (eV) for C 1s and/or O 1s core levels in Li clusters chosen to emulate adsorbed species calculated with Gaussian 94 (see text)

Species	Li cluster	C 1s	O 1s
Surface carbonate	LiOCOOLi	308.8	557.9, 557.3
$[CO_2]_{ads}$ (bent)	LiOCOLi	304.4	555.8
Superoxide	LiO_2	559.8	
Peroxide	Li_2O_2	556.9	
Oxide	Li_2O	553.8	

[a] Referenced to vacuum level.

The C 1s and O 1s spectra are changed very little upon heating to 320 K, but significant changes occur at 370 K and above. These changes are indicative of the beginning of decomposition of the surface carbonate. At 420 K, all of the surface carbonate has decomposed into elemental carbon and surface oxide. The fate of the chemisorbed CO_2 cannot be resolved based only on these spectra, i.e. whether it also decomposes to elemental carbon and oxide or desorbs intact or as CO. Likewise, we could not resolve the decomposition pathway of the surface carbonate, i.e. whether CO_2 and/or CO desorb as part of decomposition. One could resolve these questions by looking at the Li 1s to O 1s ratios, but acquisition times for Li 1s spectra of acceptable quality were excessively long.

4.3. CO_2 on lithium

As shown by the spectra in Fig. 4, multiple C and O chemical states were observed as lithium surface was exposed to CO_2 at 130 K. The spectra did not depend significantly on exposure, for dosing ranging from 10 to 40 L. To be certain that the multiple C and O states were not due to various C and O moieties caused by hot filaments, the experiments were repeated under the same conditions except that all filaments were turned off during CO_2 dosing; the resulting spectroscopic features remain the same. Curve fitting of the 130 K spectra indicated three carbon peaks and two oxygen peaks. Using the peak assignments developed in the previous section, the two peaks

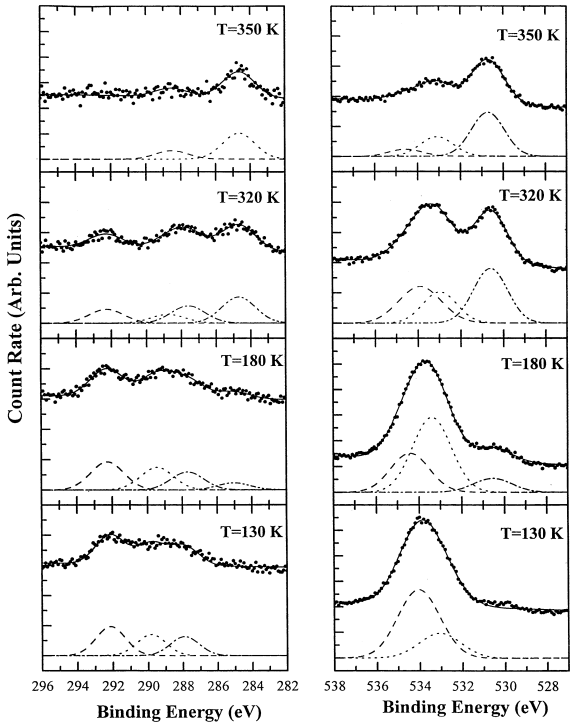

Fig. 4. Series of XP spectra of a lithium surface after 30 L CO_2 exposure at 130 K and subsequent warming to higher temperature. Solid line shows the results of peak fitting, with the individual component spectra shown as dashed, dotted and dot–dash curves.

at 292 and ca. 290 eV are assigned to surface carbonate and chemisorbed CO_2, respectively. The peak near 288 eV is 1.9 eV lower in binding energy than the peak assigned to chemisorbed CO_2. If we use transition metal carbonyls as reference compounds [24] for chemisorbed CO on Li, the expected C 1s and O 1s binding energies would be 288.0 and 534.3 eV, respectively. Thus, the C 1s state at ca. 288 eV is assigned to CO_{ads}. Surface carbonate and CO_{ads} have overlapping O 1s binding energies, and therefore there are only two features in the corresponding O 1s spectrum. For the purposes of further discussion, the experimental binding energy assignments we made for the various chemical states of C and O relevant to this study are summarized in Table 3.

The stoichiometry ratio of oxygen and carbon on the surface (in all chemical states) is a useful experimental parameter. It serves both as a method

Table 3
Experimental C1s and O1s binding energies[a] (eV) of adsorbed species on Li as assigned in this work and of related reference compounds

Species	Reference	C 1s	O 1s
Surface carbonate	this work	292.0	534.2
Chemisorbed CO_2	this work	290.0	533.2
Chemisorbed CO	this work	288.0	534.3
Li_2CO_3	[24]	289.8	531.5
$Fe(CO)_5$	[24,25]	288.0	534.3
CO	[26][b]	296	541.7
CO_2	[26][b]	297.7	540.0

[a] Referenced to C 1s for elemental carbon at 284.5 eV.
[b] Referenced to vacuum level.

of detecting gaseous products of the CO_2 reaction with Li which change the O/C stoichiometry from 2, e.g. reaction (3) with CO (gas) as a product would increase the ratio to 3, and as a test of consistency of our assignments of the XPS peaks to specific molecular species. We calculated the O/C total peak area ratios and converted them to atomic ratios using the elemental sensitivity factors for our analyzer [25]. Some caution, however, must be exercised with these values since we have neglected forward focusing effects. We know independently from ellipsometry that the Li films used in this work are non-porous and optically "smooth", i.e. high specular reflectivity, and thus photoemission from oriented molecules on this surface will not be isotropic. If CO_2 and/or CO_3^{2-} have a preferential orientation on the surface, such as standing up with C–O bonds 45° to the surface, forward focusing of O 1s electron emission along these bonds would increase the O 1s intensity at the collection angles of our analyzer in the XPS geometry. Thus, an experimental O/C ratio somewhat greater than 2 does not necessarily mean a surface stoichiometry greater than 2. Based on simulations [27] of forward focusing for a CO_2 molecule standing up on a planar surface, we concluded that an experimental ratio of 2 to 2.5 from our angle-integrated spectra would be consistent with a surface stoichiometry of 2.0.

The C1s and O 1s XP spectra evolved with increasing temperature (see Fig. 4). For convenience, the binding energies and relative fractions of each peak at various temperatures are summa-

rized in Table 4. Upon warming to 180 K, there is a dramatic rearrangement of the O 1s features, with the peaks at 534 and 533 eV essentially swapping intensities, and a new state appearing at 530.6 eV. Increasing temperatures further produces a systematic increase in intensity in the 530.5($\pm$0.2) peak and a decrease in the higher energy peaks. Since the C 1s binding energies clearly indicate the state of oxidation of the carbon atom, the chemistry behind these changes is more easily inferred from the C 1s spectra. The simplest interpretation of these spectra is the progressive decomposition of the surface CO_3^{2-} to adsorbed CO_2 and CO, and the progressive decomposition of the adsorbed CO_2 and CO to elemental carbon and oxygen (oxide) as the temperature is increased. The stoichiometric ratios of O to C calculated from the total areas of all O 1s and C 1s peaks were 2.5 ± 0.1 at all temperatures up to 320 K. As a check of self-consistency, we calculated the expected O/C ratio from the relative amounts and stoichiometries of the different molecular states of carbon assigned to each peak in the C 1s spectrum according to Table 3. At all temperatures up to 320 K, the O/C ratios thus calculated were 2.3 ± 0.1, in excellent agreement with the experimental values of the overall stoichiometries, 2.4 ± 0.1. This result would indicate that as the adsorbate layer formed at 130 K reacts further upon heating to 320 K, the reaction does not evolve a gas that changes the O/C stoichiometry, such as CO. Above 320 K, elemental carbon and oxygen (oxide) become the predominant species, and at 420 K these are the only states of carbon and oxygen on the surface. The calculated O/C stoichiometries of the surfaces above 320 K dropped to 2.2 ± 0.1. We do not believe this necessarily represents a real change in the stoichiometry of the surface, i.e. a net loss of oxygen from the surface. Another explanation is that the O 1s emission becomes more isotropic as C–O bonds are broken, and forward focusing of the O 1s emission ceases.

Table 4
Results of curve-fitting C 1s and O 1s spectra for 30 L CO_2 on Li at 130 K and subsequent warming to higher temperatures (Fig. 4)

Temperature (K)	C 1s BE (eV)	Relative peak area	O 1s BE (eV)	Relative peak area
130	292.1	0.41	534.0	0.73
	289.8	0.31	533.1	0.27
	287.9	0.27		
180	292.3	0.37	534.4	0.31
	289.4	0.30	533.4	0.59
	287.7	0.24	530.6	0.11
	285.0	0.09		
320	292.3	0.21	534.0	0.35
	288.8	0.13	533.0	0.24
	287.6	0.26	530.6	0.42
	284.7	0.40		
350	288.5	0.25	534.6	0.10
	284.7	0.75	533.1	0.28
			530.7	0.62

Of particular importance for Li batteries are the results at 320 K. To determine whether the process of dosing at 130 K followed by warming to 320 K (with about 90 min of XPS analysis time interspersed) produced the same result as direct reaction of CO_2 with clean Li at 320 K, we also obtained spectra following dosing of freshly deposited Li with 30 L CO_2 at 320 K. The resulting spectra were essentially identical to the C 1s and O 1s spectra for 320 K in Fig. 4. This result also served to confirm the absence of contamination of the surface during the relatively long total time of data acquisition.

4.4. CO on lithium

To confirm that CO formed from disproportionation of adsorbed CO_2 molecules [reaction (3)] most probably does not desorb from the Li surface, we studied the interaction of CO with clean Li using XPS. The resulting C 1s and O 1s spectra as a function of temperature following the initial 30 L dosing at 130 K are summarized in Fig. 5. The results indicate very strong reactivity of Li towards CO even at 130 K. At 130 K, three peaks are resolved in both the C 1s and O 1s spectra. Using the assignments in Table 3, we can attribute these peaks to CO_3^{2-} (292 and 534 eV), adsorbed CO (290 and 532.5 eV), elemental carbon (284.5 eV) and O^{2-} (530 eV). We observed that CO_3^{2-} forma-

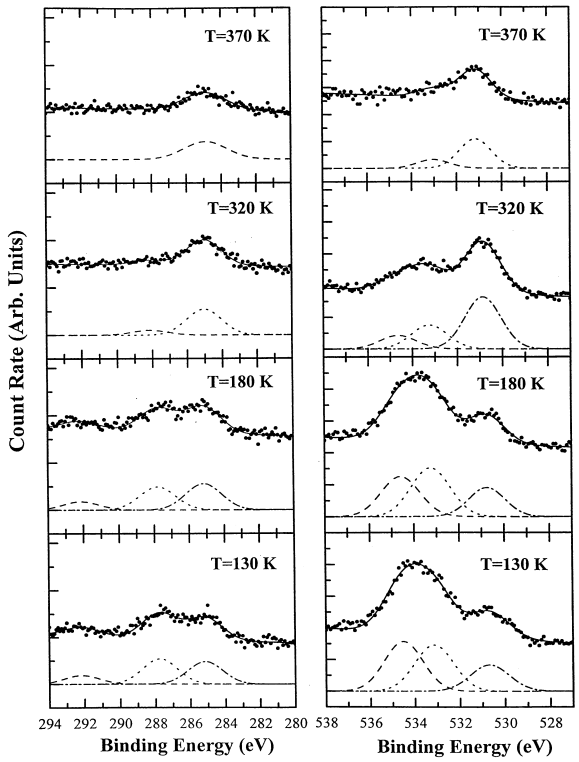

Fig. 5. Series of XP spectra of a lithium surface after 30 L CO exposure at 130 K and subsequent warming to higher temperature. Solid line shows the results of peak fitting, with the individual component spectra shown as dashed, dotted and dot–dash curves.

tion was dosage dependent, and did not occur to an observable extent at low doses, e.g. below 20 L. CO adsorption on clean Li even at 130 K then appears to be accompanied by a significant amount of dissociation to elemental carbon and O^{2-}, and further reaction of O^{2-} with CO (at sufficiently long exposures) to form CO_3^{2-}:

$$CO \Rightarrow CO_{ads} \quad (5a)$$

$$CO_{ads} \Rightarrow C + O^{2-} \quad (5b)$$

$$CO + 2O^{2-} \Rightarrow CO_3^{2-} \quad (6)$$

As this mix of adsorbates is warmed up from 130 K, both CO_3^{2-} and CO_{ads} decompose to elemental carbon and O^{2-}, which are the only species remaining on the surface at 370 K.

5. Discussion

The binding energies we have associated with various species were summarized in Table 3. These assignments were made based in part on chemical shifts obtained from Koopmans Theorem binding calculated with Gaussian 94, and in part with chemical intuition based on experimental binding energies of reference compounds. Two of these assignments differ in absolute binding energy from values reported in other studies, those for C 1s binding energy in surface CO_3^{2-} (292 eV) and adsorbed CO_2 (ca. 290 eV). The PHI Handbook [24] reports the C 1s binding energy in bulk carbonates to be 289 ± 1 eV, about 2 eV below the value we assign here for surface carbonate. We attribute this difference to a surface shift, since we are studying a surface species, probably at submonolayer coverages. The origin of this surface shift is most probably from extra-atomic relaxation [28], where a bulk CO_3^{2-} ion experiences more screening from the ionic lattice and therefore has a larger extra-atomic relaxation and lower binding energy relative to a surface ion. Studies of CO_2 adsorption on alkali metals by XPS are relatively rare (versus vibrational spectroscopies), and rarer still are XPS studies reporting C 1s spectra. In fact, we are aware of only one, by Kulkarni et al. [29], for CO_2 on Cs at 80 K. CO_2 on Cs at 80 K is reported to result in only a single state of carbon and oxygen, corresponding to a chemisorbed state of CO_2, denoted $CO_2^{\delta-}$ by Kulkarni et al. [29]. Surface carbonate was produced in the same manner as we did, by pre-dosing with oxygen followed by dosing with CO_2, all at 80 K. The binding energy assignments for the resulting surface carbonate species were ca. 291 and 533 eV. Their assignments of O 1s binding energies for O^{2-} and O_2^{2-} are in excellent agreement with ours, and their O 1s binding energies for C–O species have the same ordering from high to low, $CO_3^{2-} >$ chemisorbed $CO_2 > O^{2-}$, but with a narrower energy difference of only ca. 2 eV (versus ca. 4 eV) separating the three states. Their C 1s binding energies for surface CO_3^{2-} and chemisorbed CO_2 are about 2 eV lower than ours. These differences appear to be fundamental and attributable to the different substrate, Cs versus Li, pro-

ducing different extents of charge transfer and/or differences in extra-atomic relaxation in nominally the same surface species.

The surface chemistry of the CO_2/CO/O family on Li is quite similar to that on the other alkali metals, as summarized by Freund and Roberts [7], but with some differences as well. As on the other alkali metals, CO_2 is very reactive with surface oxygen produced by pre-dosing the surface with O_2, producing a surface carbonate species, as represented by Eq. (4). Also, all the alkali metals have in common the reaction of the clean metal surface with CO_2 to produce a surface carbonate species, even at temperatures as low as 120 K. We could not find any evidence for the direct dissociation of CO_2 on Li to form CO and O, i.e. Eq. (2), at 130 K. By inference, the carbonate formation probably proceeds via Eq. (3), the disproportionation of two chemisorbed CO_2 molecules, as proposed for Na [8,9] and K [10–12], but with adsorbed CO as the other product, i.e. the CO does not desorb from the surface. The interaction of CO with Li appears in our work to be fundamentally different from Na, K and Cs, a much stronger interaction with dissociation occurring even at 130 K. Thus, in the case of Li, adsorbed CO is an intermediate in the decomposition of surface carbonate and chemisorbed CO_2 as the temperature is raised from 130 K, a role it does not play on the other alkali metals.

The results of most relevance to Li batteries are the spectra at 320 K. The interaction of CO_2 with Li at this temperature produces a relatively small amount of surface carbonate, with the main products being elemental carbon and oxide–oxygen. The most probable reaction pathway appears to be a combination of reactions (3), (4), and (5b). In order to form a surface layer containing carbonate as the majority component, our results indicate there would have to be another source of surface oxygen in order to promote reaction (4). In a battery, the most probable source of oxygen is water, which is a ubiquitous impurity in the non-aqueous electrolyte. The interaction of water with clean Li is complex [30,31], and produces both OH^- and O^{2-} forms of surface oxygen whose relative concentrations depend on the conditions of exposure. The reactivity of CO_2 with surface oxygen from water dissociation has not yet been studied on Li by us or by any others (to our knowledge), so the interaction of CO_2 and water in the electrolyte with freshly deposited Li is difficult to predict from the present state of knowledge. Based on the results of Carley et al. for CO_2 and water on Al(111) [32], formate species in addition to the expected CO_3^{2-}/HCO_3^- species should be considered as a possibility.

6. Summary

The interaction of CO_2 with clean Li at 120–320 K was studied using photoelectron spectroscopy. To assist in the interpretation of the spectra, the C 1s and O 1s core-level binding energies of various Li cluster compounds were calculated using an ab initio SCF method. To further understand the reaction pathway, we also studied the reaction of CO_2 with an O_2 pre-dosed Li surface, and the adsorption of CO on clean Li. The principal reactions occurring between CO_2 (1–30 L) and Li at 120–320 K are:

$$CO_2 \Rightarrow [CO_2]_{ads}$$

$$2[CO_2]_{ads} \Rightarrow CO_3^{2-} + CO_{ads}$$

probably via an oxalate, $[C_2O_4]_{ads}$, intermediate, and:

$$CO_{ads} \Rightarrow C + O^{2-}$$

$$CO_2 + O^{2-} \Rightarrow CO_3^{2-}$$

The relative rates of these reactions are temperature dependent. At 120 K, the main products are CO_3^{2-}, CO_{ads}, and $[CO_2]_{ads}$, whereas at 320 K the main products are O^{2-} and elemental carbon with a relatively small amount of CO_3^{2-}. The reactions are similar to those on the other alkali metals, Na, K and Cs, with the important exception being the much stronger interaction with CO, leading to dissociation and carbon formation.

Acknowledgements

This work was supported by the Office of Energy Research, Basic Energy Sciences, Chemical

Sciences Division, of the US Department of Energy under Contract DE-AC03-76SF00098. The authors acknowledge the valuable assistance of Dr. Hubert Gasteiger and Mr. Frank Zucca in the design and construction of the UHV chamber used in this research.

References

[1] D. Aurbach, Y. Gofer, M. Ben-Zion, P. Aped, J. Electroanal. Chem. 339 (1992) 451.
[2] D. Aurbach, Y. Gofer, J. Electrochem. Soc. 128 (1991) 3529.
[3] D. Aurbach, O. Chusid, J. Electrochem. Soc. 140 (1993) L155.
[4] T. Osaka, T. Momma, T. Tajima, Y. Matsumoto, J. Electrochem. Soc. 142 (1995) 1057.
[5] T. Osaka, T. Momma, Y. Matsumoto, Y. Uchida, J. Electrochem. Soc. 144 (1997) 1709.
[6] H. Gan, E. Takeuchi, J. Power Sources 62 (1996) 45.
[7] H.-J. Freund, M.W. Roberts, Surf. Sci. Rep. 25 (1996) 225.
[8] J. Wambach, G. Ordoefer, H.-J. Freund, H. Kuhlenbeck, M. Neumann, Surf. Sci. 209 (1989) 159.
[9] S. Wohlrab, D. Ehrlich, J. Wambach, H. Kuhlenbeck, H.-J. Freund, Surf. Sci. 220 (1989) 243.
[10] F.M. Hoffmann, M.D. Weisel, J. Paul, Surf. Sci. 316 (1994) 277.
[11] Y. Shao, J. Paul, O. Axelsson, J. Phys. Chem. 97 (1993) 7652.
[12] O. Axelsson, J. Paul, M.D. Weisel, F.M. Hoffmann, J. Vac. Sci. Technol. A12 (1994) 158.
[13] G. Zhuang, K. Wang, P. Ross, Surf. Sci. 387 (1997) 199.
[14] K. Wang, P. Ross, Surf. Sci. 365 (1996) 753.
[15] P.R. Schorn, E. Hintz, S. Musso, B. Schweer, Rev. Sci. Instrum. 60 (1989) 3275.
[16] F.J. Esposto, K. Griffiths, P.R. Norton, R.S. Timsit, J. Vac. Sci. Technol. A12 (1994) 3245.
[17] M.J. Frisch, G.W. Trucks, H.B. Schlegel, P.M.W. Gill, B.G. Johnson, M.A. Robb, J.R. Cheeseman, T. Keith, G.A. Petersson, J.A. Montgomery, K. Raghavachari, M.A. Al-Laham, V.G. Zakrzewski, J.V. Ortiz, J.B. Foresman, J. Cioslowski, B.B. Stefanov, A. Nanayakkara, M. Challacombe, C.Y. Peng, P.Y. Ayala, W. Chen, M.W. Wong, J.L. Andres, E.S. Replogle, R. Gomperts, R.L. Martin, D.J. Fox, J.S. Binkley, D.J. Defrees, J. Baker, J.P. Stewart, M. Head-Gordon, C. Gonzalez, J.A. Pople, Gaussian 94 (Revision D.3).
[18] T.A. Koopmans, Physica 1 (1933) 104.
[19] L. Andrews, J. Chem. Phys. 50 (1969) 4288.
[20] S. Qiu, C. Lin, J. Chen, M. Strongin, Phys. Rev. B 39 (1989) 6194.
[21] J.A. Connor, M. Considine, I.H. Hillier, J. Chem. Soc., Faraday Trans. II 74 (1978) 1285.
[22] J.A. Connor, I.H. Hillier, V.R. Saunders, M. Barber, Mol. Phys. 23 (1972) 81.
[23] Inorganic Crystal Structure Database, Fiz. Karlsuhe and Gmelin-Institut, 1997.
[24] J. Moulder, W. Stickle, P. Sobol, K. Bomben, in: J. Chastain (Ed.), Handbook of X-ray Photoelectron Spectra, Perkin-Elmer, 1992.
[25] C. Wagner, W. Riggs, L. Davis, J. Moulder, in: G. Muilenberg (Ed.), Handbook of X-Ray Photoelectron Spectra, Perkin-Elmer, 1979.
[26] K. Siegbahn, C. Nordling, G. Johansson, J. Hedman, P.F. Heden, K. Hamrin, U. Gelius, T. Bergmark, L.O. Werme, R. Manne, Y. Bear, ESCA Applied to Free Molecules, North-Holland, Amsterdam, 1971, p. 13.
[27] J. Rehr, R. Albers, Phys. Rev. B 41 (1990) 8139.
[28] D.A. Shirley, in: M. Cardona, L. Ley (Eds.), Photoemission in Solids I, General Principles, Springer, Berlin, 1978, p. 176.
[29] G. Kulkarni, S. Laruelle, M. Roberts, J. Chem. Soc., Faraday Trans. 92 (1996) 4793.
[30] K.R. Zavadil, N.R. Armstrong, Surf. Sci. 230 (1990) 47.
[31] G. Zhuang, P. Ross, F.-P. Kong, F. McLarnon, J. Electrochem. Soc. 145 (1998) 159.
[32] A.F. Carley, P.R. Davies, E.M. Moser, M.W. Roberts, Surf. Sci. 364 (1996) L563.